Optical Engineering

OpticalEngineering.SPIEDigitalLibrary.org

Use of specklegrams background terms for speckle photography combined with phase-shifting electronic speckle pattern interferometry

Redouane Zemmamouche
Jean-François Vandenrijt
Aïcha Medjahed
Ivan de Oliveira
Marc P. Georges

SPIE.

Optical Engineering 54(8), 084110 (August 2015)

Use of specklegrams background terms for speckle photography combined with phase-shifting electronic speckle pattern interferometry

Redouane Zemmamouche,[a,*] Jean-François Vandenrijt,[b] Aïcha Medjahed,[a] Ivan de Oliveira,[c] and Marc P. Georges[b]
[a]Université Ferhat Abbas, Sétif1, Institut d'Optique et Mécanique de Précision, Laboratoire d'Optique Appliquée, Avenue Said Boukhrissa, Sétif 19000, Algeria
[b]Université de Liège, Centre Spatial de Liège, Liege Science Park, B-4031 Angleur (Liège), Belgium
[c]Universidade Estadual de Campinas (UNICAMP), Faculdade de Tecnologia/FT, Rua Paschoal Marmo 1888, CEP 13484-332, Jd. Nova Italia, Limeira, SP, Brazil

Abstract. Electronic speckle pattern interferometry (ESPI) is combined with digital speckle photography (DSP) to measure out-of-plane deformation in the presence of large in-plane translation or rotation. ESPI is used to measure out-of-plane displacements smaller than the speckle diameter. In-plane displacements larger than the speckle size are obtained by DSP using artifacts images computed from the phase-stepped specklegrams. Previous works use the specklegram modulation for that purpose, but we show that this can lead to errors in the case of low modulation. In order to avoid this, a simple averaging of phase-stepped specklegrams allows obtaining the average irradiance, which contains information on the speckled object image. The latter can be used more efficiently than the modulation in DSP and is simpler to compute. We also perform a numerical simulation of specklegrams, which show that the use of background terms is much more stable against some error sources as compared to modulation. We show experimental evidence of this in various experiments combining out-of-plane ESPI measurements with in-plane translations or rotations obtained by our DSP method. The latter has been used efficiently to restore phase loss in out-of-plane ESPI measurements due to large in-plane displacements. [DOI: 10.1117/1.OE.54.8.084110]

Keywords: speckle; digital speckle photography; speckle interferometry; electronic speckle pattern interferometry; correlation.

Paper 150692 received Jun. 11, 2015; accepted for publication Jul. 27, 2015; published online Aug. 20, 2015.

1 Introduction

Electronic speckle pattern interferometry (ESPI) is a technique used for the measurement of small deformations of diffusely reflecting objects.[1] The rough object surface is illuminated with coherent light and imaged onto a charge-coupled device (CCD) camera, where the object wave is superimposed on a reference wave. This produces a local interference pattern on the camera, the so-called specklegram. In order to measure the displacement undergone by every object point between two displaced or deformed states, specklegrams captured at these two states can be numerically subtracted from one another. This leads to an interferogram consisting of fringes superimposed on the object image. Depending on the geometrical configuration of beams, out-of-plane or in-plane measurements can be achieved.[1] In both cases, the ESPI measurement range is limited by the density of fringes, which can be resolved in the interferograms. Because the distance between two consecutive fringes is related to the laser wavelength and given the number of pixels of state-of-the-art cameras, ESPI generally allows for observing displacements up to a few tens of micrometers when used with visible lasers.

In practical applications, the object can undergo bulk motion that may be larger than the quantity to be measured by ESPI and the information between specklegrams is then lost. To overcome this problem, some techniques have been implemented. Digital speckle photography (DSP) is one of them and it is generally used to measure in-plane displacements larger than the average speckle diameter. The displacement field is calculated from the peak position of the cross correlation between subimages[2] taken from the speckle pattern of both the initial and the displaced/deformed states of the object.

In order to automatically extract quantified phase information from specklegrams, various methods are used in connection with ESPI. A first range of methods is based on phase shifting; the most commonly used method is temporal phase shifting (TPS) in which several specklegrams are acquired with additional phase steps produced between each frame.[3] Then the specklegrams are injected in a simple formula, which depends on the number of steps and on the phase step applied. Usually, the four-frame algorithm consisting of four specklegrams with $\pi/2$ phase steps is used.[3] TPS assumes that during the phase-shift acquisition, the specklegrams are not changing in both intensity and phase, which limits the method to slow object changes. Combining TPS ESPI and DSP has been used by Sjödahl and Saldner[4] to measure three-dimensional (3-D) deformation fields in out-of-plane sensitive ESPI. The authors computed the speckle modulation function of the specklegrams (the amplitude of the interference term) from the four phase-stepped images in both initial and displaced object states and then used this modulation image in DSP to obtain the in-plane

*Address all correspondence to: Redouane Zemmamouche, E-mail: rzemm@yahoo.fr

0091-3286/2015/$25.00

displacements. This method has also been used by Anderson et al.[5] to compensate for large in-plane displacements in ESPI. Groves et al.[6] have shown the combination of DSP and TPS shearography based on a Michelson interferometer. Shearography measures the out-of-plane strain components, whereas DSP measures the in-plane ones. In their setup, they used a shutter for blocking one of the interferometer arms for capturing the speckle image to be used for DSP.

Other authors used alternative methods for phase quantification and extraction of the speckle object image for DSP in cases where TPS ESPI is no longer usable, specifically for dynamic events observed with pulsed lasers.

First, the spatial phase shifting (SPS) ESPI[7] was used. In SPS, the reference beam must be tilted accurately with respect to the object beam in such a way that two adjacent pixels of the resulting specklegram have a phase shift of a given value (e.g., $\pi/2$) from one another. Then a set of three phase-shifted interferograms is obtained by calculating the spatial average of the specklegrams taken between the two instants and which are digitally shifted from one another by one pixel. These interferograms are injected in the suitable phase calculation equation (specifically the three-frame algorithm).[7] As we see, the processing is quite complex and, in addition, SPS has the limitation that speckle grains must have a lateral extension of at least 3 pixels in the direction perpendicular to the carrier fringes, which requires the use of a slit instead of a circular aperture in the imaging system.[7] Langehanenberg et al.[8] used SPS ESPI to perform out-of-plane deformation measurement. For lateral displacements, DSP was applied using the modulation terms of speckle interferograms in a similar way as in Ref. 4. SPS is also used by Martínez-Celorio et al.[9] to measure out-of-plane displacement in the presence of large in-plane displacement. In their work, they blocked the reference beam to directly record the object speckle images, without retrieving them from the set of phase-shifted images.

A second alternative to TPS is the Fourier transform (FT) method, which consists of using a carrier fringe pattern produced by tilting the reference beam with respect to the object beam. In the Fourier plane, high frequencies contain the information of phase to be used in ESPI and the low frequencies contain the background terms (reference and object beams). In that case, the speckle object field is obtained by filtering a portion of the Fourier plane. Gren[10] has shown recovery of a lost interference phase due to in-plane translation by combining pulsed ESPI with the FT method and DSP. Filtering the low frequencies and taking the inverse FT of the result allowed obtaining the speckle object image which was used for DSP, whereas higher frequencies were filtered for ESPI. The FT method requires an additional aperture for limiting the lateral extent of the different terms of interest in the Fourier plane, allowing their correct filtering but also limiting the lateral resolution of the objects observed.

In the work presented here, we have chosen to work with TPS ESPI because alternative methods have the limitations discussed above. Doing so, we assume the observation of slow object phenomena. We have seen that the combination of DSP and ESPI (whatever the phase quantification method) developed by other groups has been applied on two distinct principles. The first one consists of blocking the reference beam and separately recording images of the object covered with speckle. These images are obviously the ideal ones to be used in DSP, with the essence of the method. However, blocking the reference beam at each measurement slows down the process and requires synchronizing a shutter in the setup. The other principle is to extract an image from the sequence of phase-shifted specklegrams which contains the speckle or artifacts of the same size. So far, all works found in literature make use of the modulation of the interference term, which contains the information of the speckle of the object beam and also the reference beam. The modulation can be intrinsically low due to various factors and imperfections of the setup.

In this paper, we present a method that combines ESPI and DSP in order to study out-of-plane deformation in the presence of in-plane translations or rotations larger than the mean speckle size. Instead of blocking the reference beam or using modulation terms in the phase-stepped images, we use the background terms to calculate the in-plane displacements by DSP. We present an algorithm for compensating large in-plane rotation and translation with subpixel accuracy. This compensation is used to restore the lost information in the fringe pattern of the out-of-plane displacement. In order to confirm our approach using background terms, a comparison with the other methods is presented. We also show that using the modulation can become problematic when it is low, as is the case with a misaligned reference beam, whereas our method still provides good results.

In Sec. 2, a theoretical description of the methods for the combined ESPI and DSP is given. In Sec. 3, we present experimental results of out-of-plane ESPI measurements with phase compensation due to in-plane DSP measurements. In Sec. 4, we experimentally compare different methods for computing images for DSP based on background and modulation terms. Finally, in Sec. 5, we propose a numerical analysis of parameters of interest and their impact on each of the methods compared.

2 Theory

Figure 1 shows the optical configuration of a phase-shifting ESPI setup for measuring out-of-plane displacement, which was used in our study. A beamsplitter BS1 divides the laser light into a reference and an object beam. The smooth reference beam illuminates the CCD detector by way of a phase-stepping mirror PS. The object beam illuminates the diffusely reflecting object, and a photographic lens L images the object onto the CCD detector. It is recombined with the reference through a second beamsplitter BS2. In our experiment, the out-of-plane displacements undergone by the object will be measured by ESPI and bulk in-plane movements by DSP.

First, let us recall the principle of phase-shifting ESPI. The four-frame technique is used to calculate the phase of the deformation from the phase-stepped images. Four specklegrams are captured with the object in its initial state, with a phase step of $\pi/2$ between the reference and object beams. The irradiances of the specklegrams captured at each point (x, y) of the image plane with the initial object are given by

$$I_j(x,y) = I_{\mathrm{av}}(x,y) + I_{\mathrm{m}}(x,y)\cos\left[\varphi(x,y) + (j-1)\frac{\pi}{2}\right], \tag{1}$$

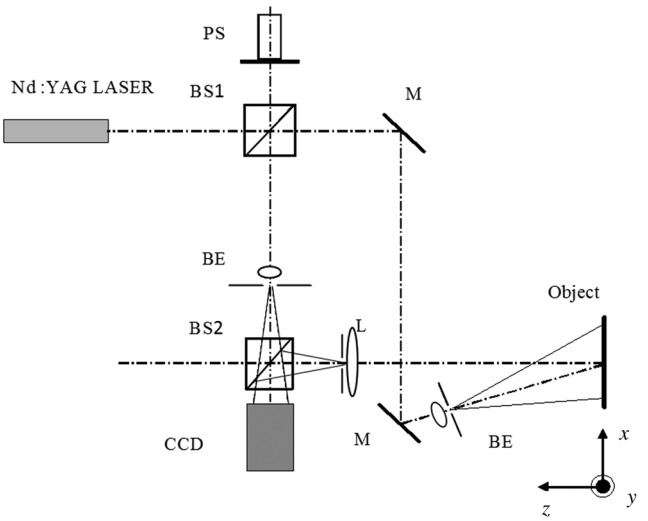

Fig. 1 Optical configuration for measurements of out-of-plane deformations. PS, phase stepped mirror; BS, beam splitter; BE, beam expander; M, mirror; SF, spatial filter; L, imaging lens; CCD, CCD camera.

where $j = 1, 2, 3, 4$. We define $I_{\mathrm{av}}(x,y) = I_{\mathrm{ref}}(x,y) + I_{\mathrm{obj}}(x,y)$ as the average specklegram irradiance (or background term), with $I_{\mathrm{ref}}(x,y)$ and $I_{\mathrm{obj}}(x,y)$, respectively, the reference and object beams irradiances, $I_{\mathrm{m}}(x,y) = 2\sqrt{I_{\mathrm{ref}}(x,y)\, I_{\mathrm{obj}}(x,y)}$, the modulation amplitude of the interference term, and $\varphi(x,y)$ is the random speckle phase given by the difference of reference and object beams' absolute phases. The phase can be computed by

$$\varphi(x,y) = \tan^{-1}\left[\frac{I_4(x,y) - I_2(x,y)}{I_1(x,y) - I_3(x,y)}\right]. \tag{2}$$

After the object has changed, four new phase-stepped images are captured:

$$I'_j(x,y) = I'_{\mathrm{av}}(x,y) + I'_{\mathrm{m}}(x,y)\cos\left[\varphi'(x,y) + (j-1)\frac{\pi}{2}\right], \tag{3}$$

where $\varphi'(x,y)$ is the phase corresponding to the new object state. Similar to Eq. (2), we can compute the phase $\varphi'(x,y)$ corresponding to the object when it is displaced or deformed.

The quantity of interest to be measured by our ESPI setup is the out-of-plane displacement $d(x,y)$ given by

$$\varphi'(x,y) - \varphi(x,y) = \frac{4\pi}{\lambda} d(x,y), \tag{4}$$

where λ is the wavelength of the laser light used.

ESPI is limited to a deformation smaller than one speckle diameter. If the in-plane deformation exceeds this, then the speckle correlation drops to zero and the information of the interference phase of the out-of-plane deformation is lost. With the use of DSP to compute the speckle displacement from the recorded images, the phase can be restored.

DSP is based on digital cross correlation between subimages in the initial and the displaced/deformed images, respectively. The cross-correlation peak position gives the statistical average of the speckle motion within the subimages. Subimages, which are used in literature[2] and in this work, have a typical size of 32×32 pixels, which is a good compromise between lateral resolution of the measurement and the cross-correlation quality. In DSP, the speckle size must be greater than 2 pixels to satisfy the sampling criteria (the Nyquist sampling criterion), which is fully satisfied by the optical configuration. The DSP measurement range is limited by the decorrelation of the speckle pattern, and the accuracy is a few percent of the pixel spacing.[4]

For measuring in-plane displacements through DSP, the phase information is not of interest. However, Sjödahl and Saldner[4] have used the modulation amplitude of the interference terms $I_{\mathrm{m}}(x,y)$ and $I'_{\mathrm{m}}(x,y)$, which are calculated from the phase stepped images by

$$I_{\mathrm{m}}(x,y) = \frac{1}{2}\sqrt{[I_1(x,y) - I_3(x,y)]^2 + [I_4(x,y) - I_2(x,y)]^2}, \tag{6}$$

$$I'_{\mathrm{m}}(x,y) = \frac{1}{2}\sqrt{[I'_1(x,y) - I'_3(x,y)]^2 + [I'_4(x,y) - I'_2(x,y)]^2}. \tag{7}$$

In the same approach, Langehanenberg et al.[8] use the modulation distribution of the specklegram proposed in Knoche et al.[11] for determining lateral displacement by DSP. In Knoche et al.,[11] six algorithms for the calculation of the specklegram modulation are described and compared. The four-step algorithm (method 3 of Ref. 11), that is convenient for our case, gives the modulation by the following:

$$\gamma(x,y) = \frac{I_{\mathrm{m}}(x,y)}{2I_{\mathrm{av}}(x,y)}. \tag{8}$$

Our approach is different. Instead of using modulation, either using Eq. (6) or its normalized form of Eq. (8), we consider the background or average irradiance $I_{\mathrm{av}}(x,y)$. In our case, two images are created from the above eight phase-stepped images $\{I_j(x,y)\}_{j=1\,\mathrm{to}\,4}$ and $\{I'_j(x,y)\}_{j=1\,\mathrm{to}\,4}$ as follows:

$$I_{\mathrm{av}}(x,y) = [I_1(x,y) + I_2(x,y) + I_3(x,y) + I_4(x,y)]/4, \tag{9}$$

$$I'_{\mathrm{av}}(x,y) = [I'_1(x,y) + I'_2(x,y) + I'_3(x,y) + I'_4(x,y)]/4. \tag{10}$$

In Sec. 4, a comparison is made between the methods using the modulation and the average irradiances.

The in-plane components of the motion between $I_{\mathrm{av}}(x,y)$ and $I'_{\mathrm{av}}(x,y)$ are calculated by DSP. Through a combination of phase-shifting ESPI and DSP, all three components of the deformation field are determined from the same recordings.

Another application of this combination, which is of interest for us in this paper, is to restore the phase lost in out-of-plane sensitive measurements by ESPI. Such losses can be due to accidental large in-plane movements and have already been observed in our practical industrial experiments. Taking a series of specklegrams and continuously computing their phase differences by Eq. (4) is performed during the object

change. When an in-plane accident occurs, the contrast of fringes is lost due to the speckle decorrelation. Then DSP is used through average irradiances obtained by the two sets of specklegrams before and after the accident. The specklegrams after the accident are recalculated on small subimages, taking into account the local movements determined by DSP.

In Sec. 3, we will present the experiments which were performed to restore out-of-plane displacement after in-plane accidental movements, using the DSP based on the average irradiances discussed earlier.

3 Experiments

In our setup (Fig. 1), the laser is a diode pumped solid state (DPSS) Nd:YAG laser with a wavelength of 532 nm and power of 400 mW from Coherent, Inc. The CCD camera is a Micam VHR 1000 with 752×582 pixels of 8.6×8.3 μm^2 pitch, and a photographic lens (L) of focal length 80 mm is used to image the object on the CCD detector. The imaging aperture is adjusted to give a speckle size of 16.7 μm typically representing 2 pixels.

The object is an aluminum plate covered with scattering white powder. For the purpose of our study, we want to provoke loss of information in out-of-plane ESPI measurements due to large in-plane movements and to restore the phase using measurements of these movements by DSP. A simple way to do this is to perform out-of-plane rotations of the object, record specklegrams at different positions, compute the interferograms by ESPI between different positions, and provoke a large in-plane movement between two sequences of specklegrams. For that purpose, the object is mounted on controllable translation and rotation stages.

The DSP processing was developed under MATLAB®. We performed the computation of $I_{av}(x, y)$ and $I'_{av}(x, y)$ [Eqs. (9) and (10)] and we kept a zone of 608×480 pixels (corresponding to a typical observed size of 28×21 mm^2), which is then decomposed into 19×15 subimages of 32×32 pixels for performing the cross correlation between $I_{av}(x, y)$ and $I'_{av}(x, y)$. From the sets of specklegrams, we computed the phase [Eq. (2)], and the difference of phases [Eq. (4)] is computed to provide out-of-plane phase maps.

A primary application of phase restoration concerns out-of-plane deformation when the object is subject to accidental in-plane translation. In an experiment, we provoked an 80 μm in-plane translation and the out-of-plane displacement consists of a rotation around the y axis. The eight phase-stepped images of the two states of the plate are recorded. The phase map of the two translations is calculated by ESPI and is shown in Fig. 2(a); the fringe contrast has decreased over the whole image. When the DSP is applied to the two sets of images as explained earlier, we obtain an in-plane displacement map presented in Fig. 2(b), with each arrow representing the local displacement on a 32×32 pixels subimage. We obtained a value of 1.641 pixels as the displacement in the x direction and 0.012 pixels in the y direction. The phase $\varphi'(x, y)$ corresponding to the second object state is then shifted by these two values. The resulting translated phase $\varphi'_t(x, y)$ is used in Eq. (4) instead of $\varphi'(x, y)$ to obtain a new restored phase map of the out-of-plane displacement, as shown in Fig. 2(c).

Another application of phase restoration concerns the case of in-plane rotations occurring during out-of-plane deformation. Figure 3(a) shows the phase map due to an out-of-plane rotation around the y axis with an in-plane rotation around the z axis of 0.7 deg. The in-plane displacement is so large in some parts of the image that the fringes were lost in these areas. Figure 3(b) shows the in-plane displacement field measured by DSP. The largest displacement is obtained in the upper right subimage and is 25.8 μm, which explains the decorrelation observed in the ESPI measurement.

Now, we will compensate the out-of-plane rotation measurement of Fig. 3(a) using the DSP results of Fig. 3(b). Compensation of the speckle movement is performed in the x and y directions with subpixel accuracy in the following.

First, we perform the compensation in the x direction by subdividing the phase image $\varphi'(x, y)$ corresponding to the deformed state of the object into rectangular horizontal strips of 608×32 pixels size. Each strip at a given y position is shifted in the x direction by the corresponding value of the displacement calculated by the DSP at their y position. Figure 3(c) shows the result of the phase compensation according to the x direction, and the lost information is restored in the lower half of the image.

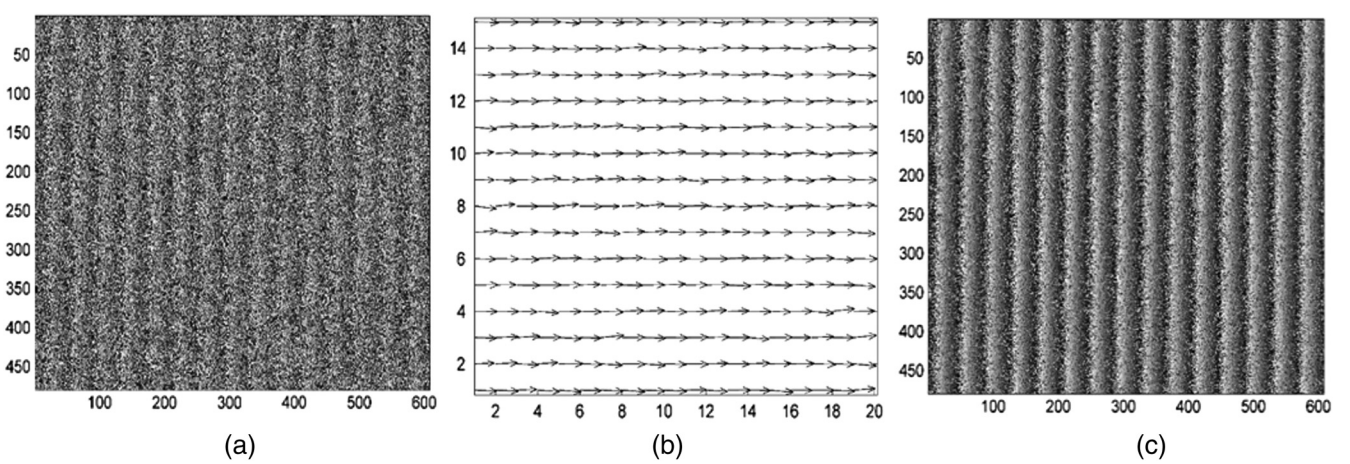

Fig. 2 Restoration of out-of-plane measurement perturbed by in-plane translation: (a) wrapped phase map of rotation obtained by electronic speckle pattern interferometry (ESPI), (b) in-plane translation obtained with digital speckle photography (DSP), and (c) restored ESPI phase map in the x and y directions.

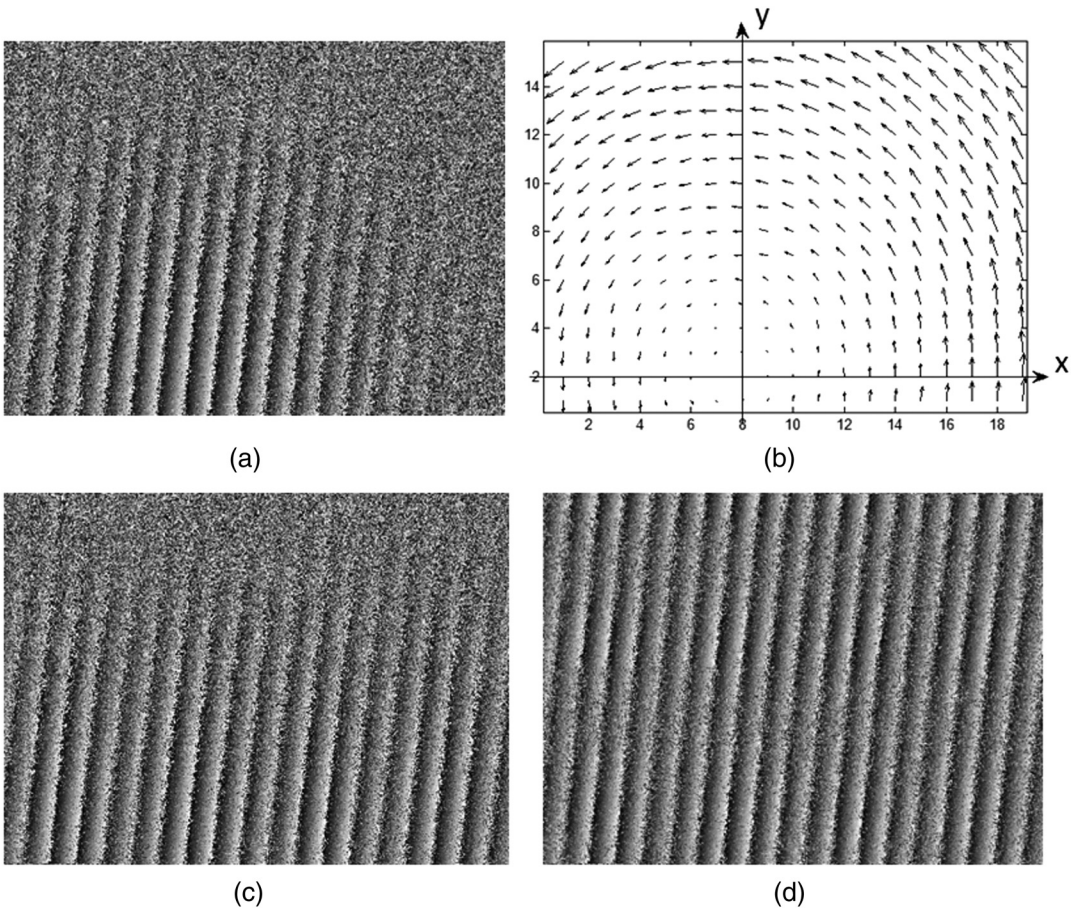

Fig. 3 Restoration of out-of-plane measurement perturbed by in-plane rotation: (a) wrapped phase map obtained by ESPI, (b) deformation field obtained with DSP, (c) restored phase map in the *x* direction when the information from (b) is used, and (d) restored phase map in the *x* and *y* directions.

Subsequently, we compensate in the y direction in the same way but, in this case, we subdivide the phase map already compensated [Fig. 3(c)] along x into vertical strips of 32×480 pixels size. Figure 3(d) shows the final result of compensation in the x and y directions, where we can see that the fringe pattern is completely restored.

Now, we are interested in comparing the method using the average irradiance of the four phase-stepped specklegrams I_{av}, which is used as an artifact image for implementing DSP in the restoration of phase after a large in-plane accident.

4 Comparison of Methods for Producing Speckle Images for DSP

This part of the work is devoted to a comparison of methods, which provide images to be used in the cross-correlation algorithm of the DSP. We establish a comparison between the methods described in Sec. 2 and another method that will be introduced. We remind the reader that in our case, we use the average irradiance $I_{\mathrm{av}}(x,y)$ taken from the set of phase-stepped specklegrams. Other works mainly made use of the modulation of the interference term $I_{\mathrm{m}}(x,y)$ [Eq. (6)], a normalized version of this last modulation $\gamma(x,y)$ [Eq. (8)] or directly using the speckled object image $I_{\mathrm{obj}}(x,y)$ obtained after blocking the reference beam. In fact, the ideal method is the latter because only the speckle generated by the object is necessary in principle for the cross correlation. However, when DSP is used in combination with phase shifting ESPI, the "I_{obj} method" would require a preliminary acquisition of only the object image with the reference beam blocked before each phase-shifted specklegram sequence, which is disadvantageous in practice and is time consuming.

We now reach the main discussion point of this section: using $I_{\mathrm{m}}(x,y)$ or $\gamma(x,y)$ could be a problem in DSP in the case of low modulation of the interference term in Eq. (1). Let us remark that Eq. (1) is an idealized case where the modulation only depends on the irradiances of the reference and object beams. In fact, the modulation can be impacted by several factors. The first factor is well known in interferometry and is the difference in polarizations between the interfering beams. Equation (1) is valid for identical polarizations, which is not always the case in practice, e.g., when an object depolarizes light which further interferes with a reference beam linearly polarized. A second factor is the integration of speckle grains in a pixel. This was discussed by Maack et al.[12] and they show that the higher the number of speckle grains integrated on a pixel, the lower the modulation. However, this is not an issue here since we have to resolve the pixel in order to apply DSP. A third factor is the matching of wavefronts between reference and object beams, as is known and largely discussed in literature.[13,14] Various reference beam configurations exist with advantages and drawbacks,[14] but the usual case is the one of the smooth

reference beam, which is used in our setup. For a typical ESPI arrangement as presented in Fig. 1, the reference beam and the object beam arise from conjugate points: the reference beam is a spherical wave coming from a point source formed by a microscope objective lens (and possibly filtered spatially) and the object beam arises from the center of the diaphragm of the imaging lens L. Therefore, both wavefronts match quite well and the modulation I_m is maximal. An important question that comes here is what happens if the modulation is low due to unmatched polarizations and/or wavefronts? In order to discuss this modulation decrease, we need to introduce a coefficient κ in Eq. (1), which contains different contributions to the modulation listed above. We then rewrite Eq. (1) as follows:

$$I_j(x,y) = I_{av}(x,y) + 2\,\kappa(x,y)\,\sqrt{I_{ref}(x,y)\,I_{obj}(x,y)} \times \cos\left[\varphi(x,y) + (j-1)\frac{\pi}{2}\right], \tag{11}$$

with κ defined by

$$\kappa(x,y) = \frac{I_m(x,y)}{2\sqrt{I_{ref}(x,y)\,I_{obj}(x,y)}}. \tag{12}$$

In order to decrease the modulation of the cosine term, a simple way to proceed experimentally is to misalign the reference beam, causing a mismatch between the reference and object wavefronts. We will analyze how the different methods behave for extracting artifacts to be used in DSP.

Figure 4 shows the comparison of images that can be used for that purpose. Figure 4(a) is $I_{obj}(x,y)$, which is taken after blocking the reference beam. This image is obviously considered as the ideal one for DSP and is the one to which we will compare other methods. Figure 4(b) is the average intensity computed from Eq. (9). The speckle is clearly obtained but the imprint of the reference beam is observed. Although a reference beam with such inhomogeneity does not highly impact the quality of ESPI results, it could impact the performance of the I_{av} method for DSP. For that reason, we now introduce another method, which consists of retrieving the reference beam image $I_{ref}(x,y)$ from $I_{av}(x,y)$, which by definition gives $I_{obj}(x,y)$. This procedure requires a single preliminary capture of $I_{ref}(x,y)$, but only once prior to all the measurements, contrary to the I_{obj} method, which requires preliminary capture prior to each phase-stepped sequence. This new method supposes that the reference beam intensity does not vary during all the measurements. Figure 4(c) shows the result of this subtraction, which looks quite similar to $I_{obj}(x,y)$. Figure 4(d) shows $I_m(x,y)$ and Fig. 4(e) shows $\gamma(x,y)$, which are similar to one another and also present variations similar to $I_{av}(x,y)$.

If we now alter the setup, e.g., by tilting the reference beam by an angle θ from the optical axis, the reference and object beams do not match perfectly and the modulation of their interference decreases. In general, this has a low impact in phase-stepping ESPI measurements. However, if we want to apply DSP under such a misaligned system, we can compare the effect of such a decrease of the modulation. Figure 5 shows the image obtained with the different methods already compared in Fig. 4 but here with a misaligned setup, at an angle $\theta = 10$ deg. We have also taken similar images at the intermediate angle $\theta = 6$ deg. The coefficient κ can be computed through Eq. (12), using separate captures of $I_{obj}(x,y)$ and $I_{ref}(x,y)$, as well as the image $I_m(x,y)$ computed by Eq. (6). In fact, $\kappa(x,y)$ depends on the

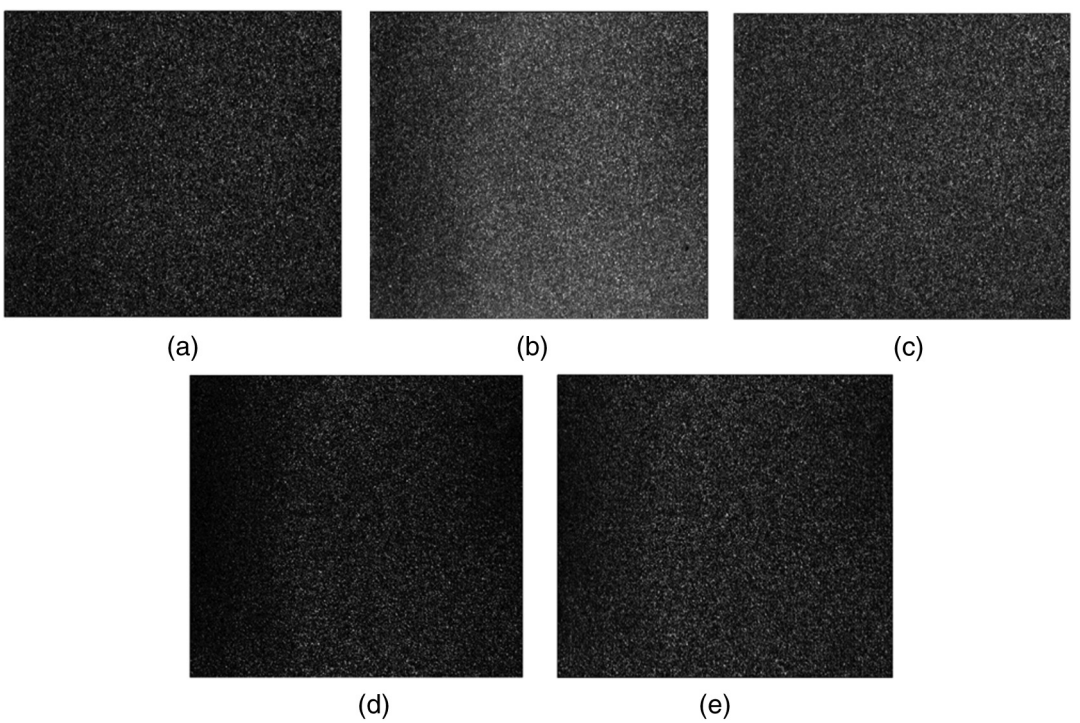

Fig. 4 Images used for cross correlation in the case of well aligned beams. Comparison of five methods: (a) I_{obj}, (b) I_{av}, (c) $I_{av} - I_{ref}$, (d) I_m, and (e) γ.

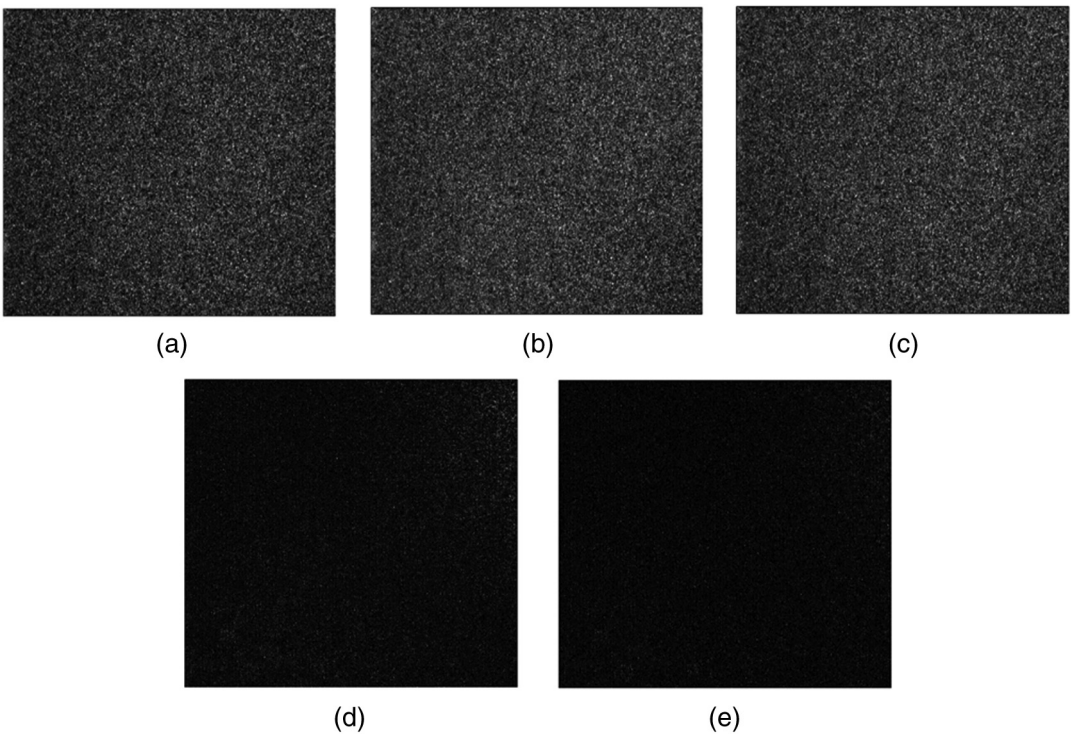

Fig. 5 Images used for cross-correlation in the case of misaligned beams. Comparison of five methods: (a) I_{obj}, (b) I_{av}, (c) $I_{av} - I_{ref}$, (d) I_m, and (e) γ.

location in the image. So we compute its average κ based on the average of $I_m(x, y)$. The different values of $\langle I_m(x, y)\rangle$ and κ are given in Table 1.

It can be clearly observed that the images based on modulation [Figs. 5(d) and 5(e)] have a much lower intensity than others [Figs. 5(a)–5(c)] and the speckle artifacts are less visible, too. Therefore, in principle, DSP results using modulation should be altered. We then performed an experiment consisting of in-plane translation and computed the global displacement by DSP. We have compared the five methods presented above, and additionally in the two cases where the object and reference beams are well aligned and then misaligned. Figure 6 presents the computed in-plane displacement for the case of the $\theta = 10$ deg misalignment angle. It can be seen that methods based on I_{obj}, I_{av}, and $I_{av} - I_{ref}$ give similar results: all the displacement computed on the different subimages goes in the same direction with the same amplitude. In the case of methods based on the modulation, I_m and γ, a large number of erroneous results is obtained: arrows have random directions and lengths. It must be noted that the arrow plots are obtained by autoscaling the vector displacements calculated by DSP. Such erroneous values are not observed in the case of a well aligned ESPI setup. The example is shown in Fig. 3, which was obtained with a well aligned reference, and object beams did not show any difference between the different methods on a similar in-plane movement.

Table 1 Values of average modulation and coefficient κ for different misalignment angles between reference and object beams.

Misalignment angle θ (deg)	$I_m(x, y)$	κ
0	30 ± 13	0.3 ± 0.13
6	8 ± 4.4	0.13 ± 0.09
10	3 ± 1.4	0.07 ± 0.07

Table 2 shows values of displacements in pixels obtained by DSP in the different cases discussed earlier. The same experiment of in-plane translation has been performed in the case of a well aligned setup and then with misaligned ones, with increasing the levels of misalignment, hence decreasing values of the coefficient κ. The displacements are expressed in pixels, as computed by the cross-correlation software. They represent the average value of the displacement measured for each of the 19×15 subimages; the standard deviation is also given in the table. We also calculated the relative error (in percent) of these displacements with respect to that calculated by the ideal I_{obj} method.

It can be seen that in the case of well aligned beams, all methods give results which are in good agreement with the I_{obj} method. In the case of a misaligned setup, good results are obtained with I_{av} and $I_{av} - I_{ref}$ methods. However, I_m and γ methods provide average values, which depart from I_{obj} when the misalignment increases and the standard deviation is dramatically high for a misalignment of 10 deg, which make these methods unreliable for DSP in this case.

We performed similar experiments with in-plane rotations and computed the displacements by DSP in the case of the misaligned setup (Fig. 7). It is clear that I_m and γ methods fail again as is observed in Figs. 7(d) and 7(e). Also, it can be observed that the I_{av} method provides some erroneous values [Fig. 7(b)], which are removed when a preliminary image of the reference beam is subtracted [Fig. 7(c)].

We applied the restoration of phase already discussed in Sec. 3 to the case of the misaligned setup ($\theta = 10$ deg). We

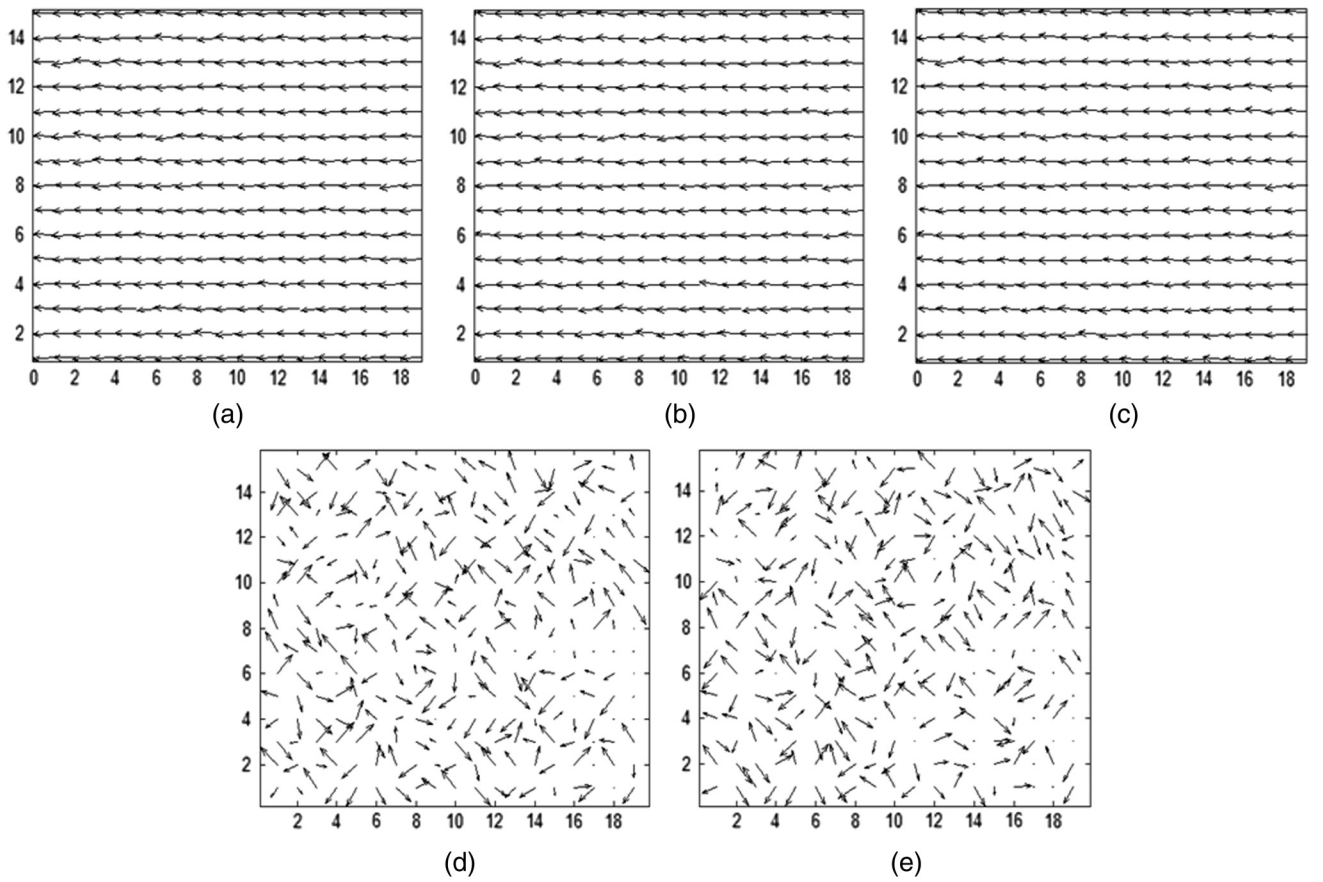

Fig. 6 In-plane translation fields obtained with DSP in the case of misaligned beams by five methods: (a) I_{obj}, (b) I_{av}, (c) $I_{av} - I_{ref}$, (d) I_m, and (e) γ.

Table 2 Comparison of methods for digital speckle photography (DSP) in the case of well aligned and misaligned object and reference beams.

	Well aligned beams $\theta = 0$ deg ($\kappa = 0.3$)		Misaligned beams $\theta = 6$ deg ($\kappa = 0.13$)		Misaligned beams $\theta = 10$ deg ($\kappa = 0.07$)	
Method	Displacement in pixel	Error (%) Relative to I_{obj}	Displacement in pixel	Error (%) Relative to I_{obj}	Displacement in pixel	Error (%) Relative to I_{obj}
I_{obj}	-1.104 ± 0.049	—	-1.080 ± 0.050	—	-1.096 ± 0.047	—
I_{av}	-1.065 ± 0.064	3.9	-1.053 ± 0.076	2.7	-1.075 ± 0.052	2.1
$I_{av} - I_{ref}$	-1.098 ± 0.052	0.6	-1.087 ± 0.058	0.7	-1.08 ± 0.052	1.6
I_m	-1.100 ± 0.061	0.4	-1.072 ± 1.843	0.8	-2.20 ± 18.07	Not reliable
γ	-1.095 ± 0.06	0.9	-0.974 ± 1.406	10.6	-0.106 ± 8.24	Not reliable

reproduced the experiment of Fig. 3: an out-of-plane rotation has to be measured by phase-shifting ESPI but is perturbed by an in-plane rotation that we measure by DSP. Figure 8(a) shows the phase map of an out-of-plane rotation obtained by ESPI. Similar to Fig. 3(a), fringes are lost where the displacement due to the in-plane rotation is high, i.e., far from the rotation center. Additionally, the contrast of fringes in the bottom left corner of the image is lower here due to the misaligned setup. The DSP is now applied using images calculated by the $I_{av} - I_{ref}$ method, which was the most efficient, as shown in Fig. 7. The in-plane displacement measured by DSP is shown in Fig. 8(b). These displacements are used to restore the phase by the method already explained in the previous section. The resulting phase map is shown in Fig. 8(c).

5 Numerical Analysis of the Effect of Parameters of Interest

In order to summarize the experimental results presented at the previous section, we have seen that DSP, based on the modulation extracted from the phase-shifted specklegrams, can return unreliable results when the modulation (hence the κ coefficient) is low. The ideal κ is equal to one, but

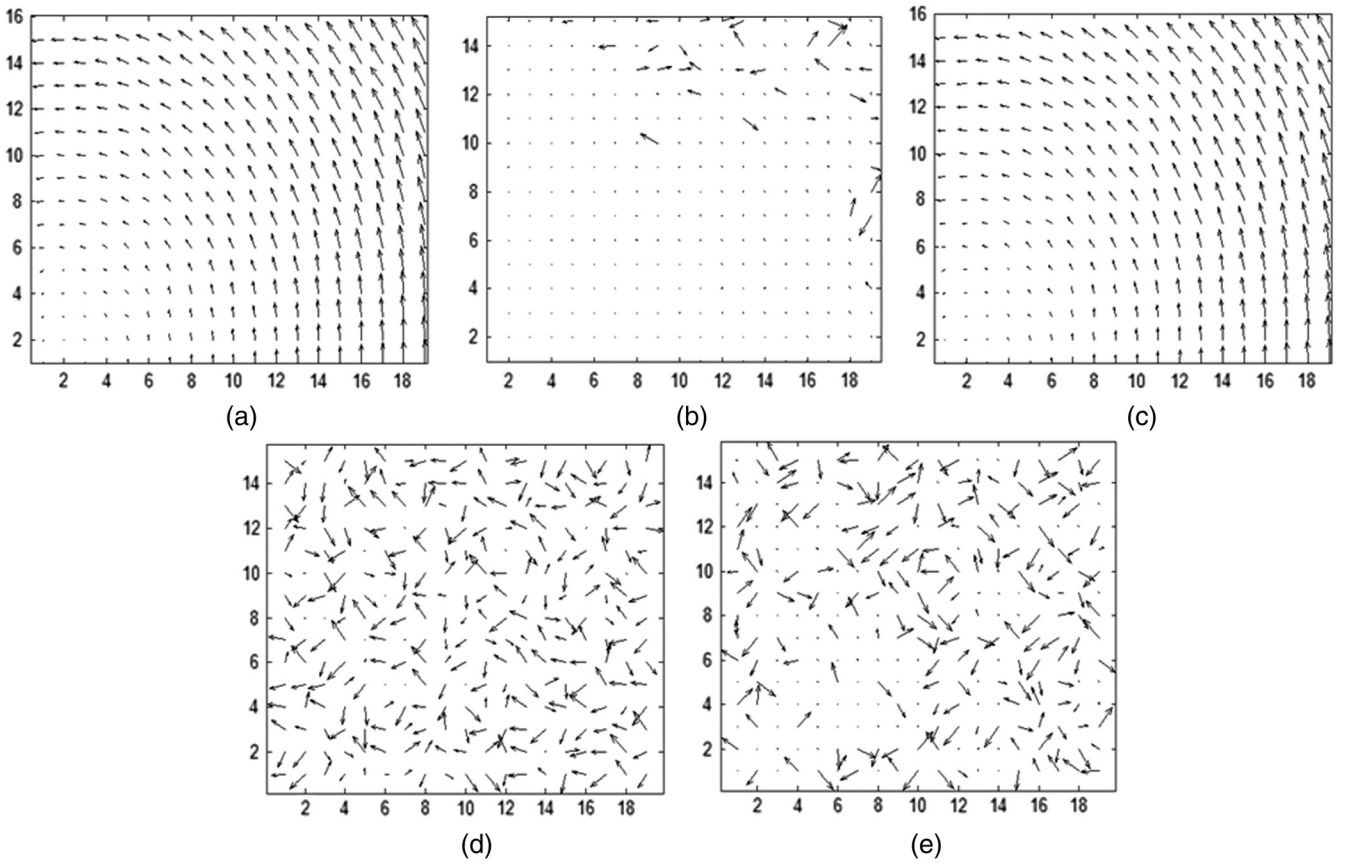

Fig. 7 In-plane rotation fields obtained with DSP in the case of misaligned beams by five methods: (a) I_{obj}, (b) I_{av}, (c) $I_{av} - I_{ref}$, (d) I_m, and (e) γ.

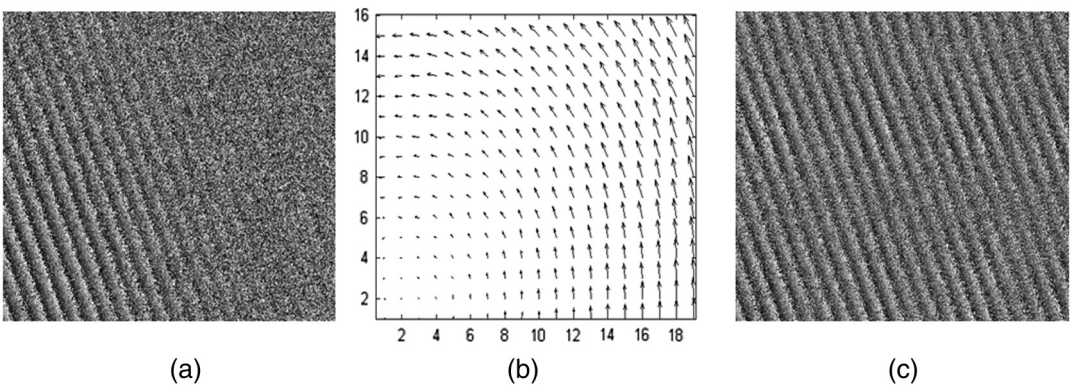

Fig. 8 Restoration of out-of-plane measurement perturbed by in-plane rotation in the case of misaligned setup: (a) wrapped phase map obtained by ESPI, (b) deformation field obtained with DSP, and (c) restored phase map in the x and y directions.

in practice, it has smaller values. For the best alignment, which we were able to reach so far in our setup, an average value of κ was determined to be on the order of 0.3 (Table 1). We have seen that under such circumstances, the different methods show good agreement with one another. When the κ value is smaller, the methods based on modulation (I_m and γ) show an increase of errors, with higher errors for the second one, while methods based on background terms (I_{av} and $I_{av} - I_{ref}$) still return good results.

We will now analyze the parameters which influence the capability of each method to be used in DSP, i.e., to stay consistent (or as close as possible) to the real speckled object image I_{obj}, which is the ideal one for DSP. In the following, we have numerically simulated specklegrams by using Eq. (11), not considering a full image but a line of 200 pixels, which is found sufficiently good while allowing a short computing time. The object beam irradiance I_{obj} is simulated with a random speckle of 2 pixels lateral extent, which corresponds to our experimental speckle size. The smooth reference beam I_{ref} is simply a constant value (spatially filtered beam without speckle). In practice, the reference beam can show some variations (e.g., Gaussian profile), but we have

neglected them here for simplicity, and this corresponds sufficiently to our reference beam. The phase φ was set to a value which yields close and resolvable fringes. In order to be consistent to the real experimental results, we have truncated the simulated values to integers ranged between 0 and 255 (digitalization on 8 bits). For simulating values of κ, we also use a random pattern but with parameters which are such that its average and deviation are the ones observed experimentally and given in Table 1. Since we use random patterns, all simulations presented in this section were performed 20 times and the figures of merit of interest calculated in various cases are averaged values. In all cases, standard deviations were on the order of 2%.

First, we have simulated the case of a well aligned system (angle between reference and object beam $\theta = 0$ deg, which corresponds to $\kappa = 0.3$). We also used typical irradiance values of our experimental object and reference beams and our simulation returned the profile of I_{obj} plotted in Fig. 9(a), together with the constant smooth reference object irradiance I_{ref}. From these two sets of values, we can compute I_{av}, $I_{\text{av}} - I_{\text{ref}}$, I_{m}, and γ. Figures 9(b)–9(d) show, respectively, $I_{\text{av}} - I_{\text{ref}}$ calculated by Eq. (9), I_{m} by Eq. (6), and γ by Eq. (8) (we have omitted displaying I_{av} for simplicity). We can see that as expected, $I_{\text{av}} - I_{\text{ref}}$ returns a pattern similar to I_{obj}. The computed values of I_{m} are in good agreement with those obtained experimentally, which comforted us in our simulation approach. The plot of I_{m} shows many artifacts, sufficiently distinguished to be used for DSP and with some similarities with I_{obj}. The values of γ (ranged between 0 and 1) are relatively low, but artifacts are also observed but with less similarity to I_{obj}.

In order to objectively analyze the similarity of all these plots with I_{obj}, we will compute the correlation coefficient r between each of them and I_{obj}, which is defined as follows:

$$r_X = \frac{\sum_{i=1}^{n}(X_i - \langle X\rangle)(I_{\text{obj},i} - \langle I_{\text{obj}}\rangle)}{\sqrt{\sum_{i=1}^{n}(X_i - \langle X\rangle)^2 \sum_{i=1}^{n}(I_{\text{obj},i} - \langle I_{\text{obj}}\rangle)^2}}, \tag{13}$$

where n is the number of pixels simulated (here 200) and X represents I_{av}, $I_{\text{av}} - I_{\text{ref}}$, I_{m}, or γ. In the case of the simulations shown in Fig. 9 and corresponding to $\kappa = 0.3$, we obtain the values in Table 3. We can see that the first two methods based on background terms are perfectly correlated to I_{obj}, whereas I_{m} and γ are, respectively, moderately and weakly correlated to the latter.

Now, we will study the influence of some parameters of interest. First, as we make use of phase-shifted specklegrams, we analyze the effect of an error on the phase step for the different methods. The four-frame algorithm, which is used here, assumes a phase step of $\pi/2$ [Eq. (2)]. As is known in interferometry, if a phase step different to this value is applied (e.g., coming from a bad calibration of the phase shifter), then error appears on the calculated phase.[15] In our simulation, we have introduced a multiplicative error coefficient to the $\pi/2$ phase step in the cosine term of Eq. (11). We have simulated a relative error ranging between 0% and 50%. The resulting correlation coefficients for the four methods are plotted in Fig. 10.

We can see that both methods based on background terms give a maximal correlation coefficient of 1 for small errors, which decreases to 0.99 for phase-shift errors larger than 10%. I_{m} decreases from the maximal value of 0.78 to 0.65 for a phase-shift error of 50%, while γ remains low and unchanged, close to its value of Table 3. It must be noted that, in practice, errors of a few tens of percents in phase-shifting are not observed when a correct phase-shifter calibration is performed. One may conclude that phase-shifting errors produce a very limited impact on the performance of all the methods studied.

We have also studied the effect of additive noise I_n in the background term. In order to take it into account in Eq. (11), we write $I_{\text{av}} = I_{\text{obj}} + I_{\text{ref}} + I_n$. Such noise can come from incoherent background light and does not participate in the specklegram interference term, but it decreases its contrast. This additive noise will be obviously present in methods based on I_{av}, $I_{\text{av}} - I_{\text{ref}}$ and γ but not in I_{m}, through their definition. We have simulated I_n, which is expressed in

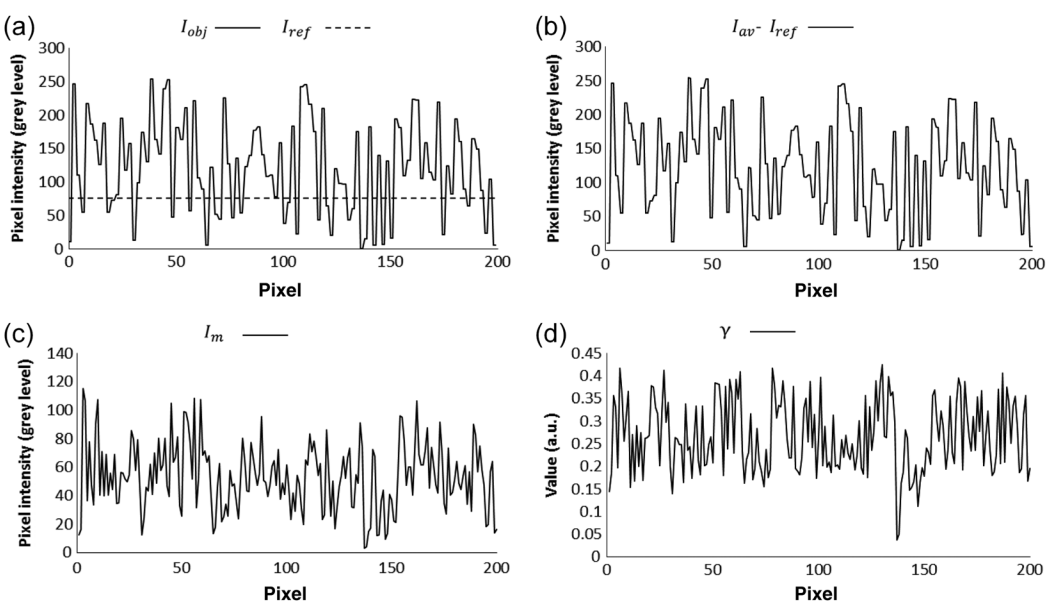

Fig. 9 Simulation of (a) I_{obj} and I_{ref}, (b) $I_{\text{av}} - I_{\text{ref}}$, (c) I_{m}, and (d) γ.

Table 3 Correlation coefficient between I_{obj} and the four methods used in DSP for $\kappa = 0.3$.

Method, X	r_X
I_{av}	1
$I_{av} - I_{ref}$	1
I_m	0.78
γ	0.12

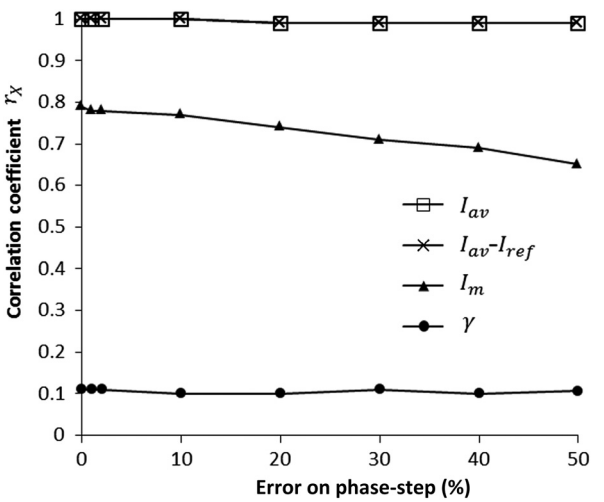

Fig. 10 Evolution of the correlation coefficient between I_{obj} and different methods used in DSP in function of relative error on the phase step (in the case of the four-frame algorithm).

percentage of the average irradiance $I_{obj} + I_{ref}$. Figure 11 shows the evolution of the correlation coefficient between each method and I_{obj} when the percentage of noise increases up to 100%. It is clear that such noise has a negligible effect.

Finally, we have studied the effect of the beam ratio R between I_{ref} and I_{obj}. We have performed the simulations by changing the level of I_{ref}, hence of R, and the simulation was reproduced for different values of experimental values of κ (Table 1). Additionally, we used an ideal value κ of 1 with no deviation. Simulations for all values of κ show the same behavior, which is presented in Fig. 12(a), in the case of $\kappa = 0.3$. Methods based on background terms return a perfect correlation to I_{obj}, whatever the ratio R. I_m shows a lower but constant correlation and γ shows a correlation which, for increasing values of R, tends asymptotically to a maximal value $r_{\gamma,max}$, which is equal to the one of I_m. Figure 12(b) shows the influence of κ on the maximal coefficient of correlation $r_{X,max}$ for each method X.

From the above numerical study, we can conclude that the methods based on background terms always show a perfect correlation with the ideal I_{obj} method. The other methods based on the modulation have a lower correlation, specifically the γ method. Increasing the ratio R significantly improves the γ method, but doing so will degrade the specklegram contrast, which is not advantageous for the combined ESPI. At last, it is clear that all methods will behave well and similarly to one another when the coefficient κ reaches its

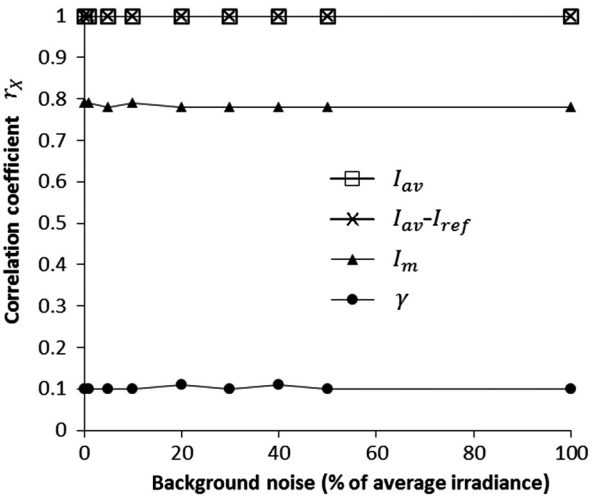

Fig. 11 Evolution of the correlation coefficient between I_{obj} and different methods used in DSP in function of incoherent background noise (in the case of the four-frame algorithm).

maximal value. This is the case of a perfectly aligned setup and with identical polarizations of the reference and object beams.

6 Discussion and Conclusion

In this work, we have discussed a method for simultaneous measurement of three components of the displacement/deformation field from the phase-stepped specklegrams acquired by temporal phase-shifting ESPI and combined with DSP. Out-of-plane displacements smaller than the speckle size are determined by ESPI, while DSP computes in-plane-displacements larger than the speckle size. DSP performs the cross-correlation between images of the object, taken prior to and after the object movement, and which are covered with speckle grains sufficiently resolved. When applying DSP in combination with out-of-plane ESPI, one way to achieve this is to block the reference beam of the ESPI setup and capture the speckle image at each position of the object prior to the phase-stepped sequence. The other way is to make use of the phase-stepped specklegrams recorded at each object position during its deformation/movement, which allow obtaining images with artifacts from which DSP is applied. This has been reported already by other authors, who use the specklegrams' modulation (amplitude of interference term) for that purpose.

In our paper, we have proposed a simpler method based on the average of the phase-stepped specklegrams (background term), which is a straightforward addition of images. Besides the obvious advantage that the average is much simpler to compute than the modulation, we show that the average method is immune against errors observed with the modulation. Such errors are prominent when the specklegram modulation is low, as is the case when the polarizations and/or wavefronts of object and reference beams are badly matched. In the case of polarizations, this can be caused by the object surface properties and cannot necessarily be controlled. The wavefronts mismatch is caused by setup imperfections or misalignment.

We have shown experimentally the impact of a setup misalignment in the application of DSP combined with ESPI. While out-of-plane ESPI interferograms were of correct

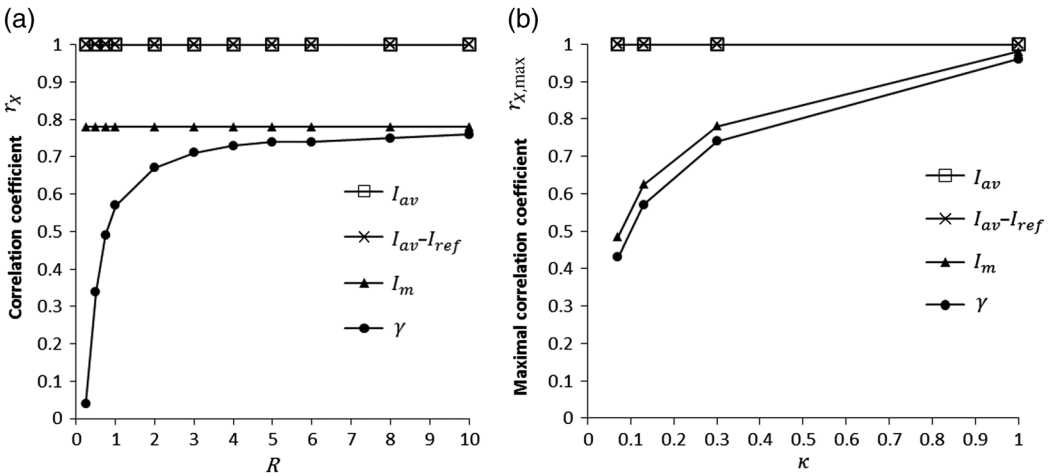

Fig. 12 (a) Evolution of the correlation coefficient between I_{obj} and different methods used in DSP in function of ratio R (in the case of the four-frame algorithm) and (b) maximal correlation coefficient in function of κ.

quality, the extraction of speckle images through the specklegram modulation failed to give reliable results in in-plane measurements by DSP. On the contrary, using the background terms still made this measurement feasible. We have also shown that a preliminary capture of the reference beam image can be retrieved from all average images to further improve the performance of the method.

We have numerically studied some parameters of interest, which could have an impact on the different methods for their proper use in DSP, i.e., we have studied the correlation between the ideal method (which uses the image of the object covered with speckle) and all methods extracting features from the phase-stepped specklegram sequences. In particular, we found no effect of an incoherent additive noise on any of the methods, based either on background terms or on modulation of specklegrams. An error on the phase step had no effect on most of the methods and an insignificant one on the modulation method. We found a significant effect of the ratio between the reference and object beams on one of the methods based on modulation. When the reference beam irradiance becomes much higher than the object one, all methods tend to behave similarly. Also, we have shown that when the intrinsic modulation increases (high values of the merit coefficient κ), all methods behave similarly and should return reliable in-plane DSP measurements.

Compared to works already published on the combined in-plane DSP and out-of-plane ESPI measurements, the measurement range obtained is consistent with other works. There is a priori no reason that the in-plane DSP measurement based on background terms returns different results than using modulation. However, it is clear that methods based on the modulation have to be used when the latter is high, otherwise DSP fails. Therefore, we recommend using the simpler method based on the specklegrams' background term.

With this method, we have performed experiments of out-of-plane measurements by ESPI, which were perturbed by an accidental large in-plane movement (rotation) and in the case of a misaligned setup. The restoration of the out-of-plane phase map through in-plane DSP measurements and based on the average of specklegrams proved to be working efficiently.

The application of this in future works will be to correct in-plane accidental movements which perturb or provoke loss of phase during measurement by out-of-plane sensitive ESPI, as is sometimes the case in out-of-laboratory conditions.

Acknowledgments

Redouanne Zemmamouche would like to acknowledge the Ministry of Higher Education and Scientific Research of Algeria, the University of M'SILA, and the Institut National d'Optique et Mécanique de Precision of Sétif University for providing the grant for his internship to the Centre Spatial de Liège (Université de Liège). He is very grateful to Dr. Marc Georges for his valuable help to achieve this work. Ivan de Oliveira would like to acknowledge the Fundação de Amparo à Pesquisa do Estado de São Paulo (FAPESP) for providing funding during his postdoctoral position at the Centre Spatial de Liège (Université de Liège).

References

1. T. Kreis, *Handbook of Holographic Interferometry—Optical and Digital Methods*, Wiley-VCH, Weinheim, Germany (2005).
2. M. Sjödahl and L. R. Benckert, "Electronic speckle photography: analysis of an algorithm giving the displacement with subpixel accuracy," *Appl. Opt.* **32**, 2278–2284 (1993).
3. K. Creath, "Phase-shifting speckle interferometry," *Appl. Opt.* **24**, 3053–3058 (1985).
4. M. Sjödahl and H. O. Saldner, "Three-dimensional deformation field measurements with simultaneous TV holography and electronic speckle photography," *Appl. Opt.* **36**, 3645–3648 (1997).
5. A. Andersson, A. Runnemalm, and M. Sjödahl, "Digital speckle pattern interferometry: fringe retrieval for large in-plane deformations with digital speckle photography," *Appl. Opt.* **38**, 5408–5412 (1999).
6. R. M. Groves et al., "Single-axis combined shearography and digital speckle photography instrument for full surface strain characterization," *Opt. Eng.* **44**(2), 025602 (2005).
7. G. Pedrini, B. Pfister, and H. Tiziani, "Double pulse-electronic speckle interferometry," *J. Mod. Opt.* **40** (1), 89–96 (1993).
8. P. Langehanenberg et al., "Detection of 3D-displacements by application of digital correlation technique and spatial phase shifting electronic speckle-pattern interferometry (SPS ESPI)," in *DGaO-Proceedings* [online only], Vol. 105, p. P35 (2004).
9. R. A. Martínez-Celorioa et al., "Out-of-plane displacement measurement by electronic speckle pattern interferometry in presence of large in-plane displacement," *Opt. Comm.* **208**, 17–24 (2002).
10. P. Gren, "Pulsed TV holography combined with digital speckle photography restores lost interference phase," *Appl. Opt.* **40**, 2304–2309 (2001).
11. S. Knoche et al., "Modulation analysis in spatial phase shifting electronic speckle pattern interferometry and application for automated

data selection on biological specimens," *Opt. Commun.* **270**, 68–78 (2007).
12. T. Maack, R. Kowarschik, and G. Notni, "Optimum lens aperture in phase-shifting speckle interferometric setups for maximum accuracy of phase measurement," *Appl. Opt.* **36**, 6217–6224 (1997).
13. R. Jones and C. Wykes, *Holographic and Speckle Interferometry*, 2nd ed., Cambridge University Press, Cambridge, United Kingdom (1989).
14. M. Lehmann, "Optimization of wavefield intensities in phase-shifting speckle interferometry," *Opt. Commun.* **118**, 199–206 (1995).
15. K. Creath, "Temporal phase measurement methods," in *Interferogram Analysis: Digital Fringe Pattern Measurement Techniques*, D. W. Robinson and G. T. Reid, Eds., pp. 94–140, Institute of Physics Publishing, Bristol, United Kingdom (1993).

Redouane Zemmamouche has been an assistant professor at the University of Mohamed Boudiaf M'SILA at the Institute of Mechanics since 2004. He received his Magistère degrees in technical optics from the Institut d'Optique et Mécanique de Précision University of Ferhat Abbas Sétif, Algeria in 2001. His current research interest is speckle metrology.

Jean-François Vandenrijt received a PhD degree in engineering from the University of Liège (Belgium) in 2010. He is an optical engineer at the Centre Spatial de Liège (CSL) in the Laser and NDT Laboratory. His research focuses on the development of optical metrological instruments in the visible and thermal infrared spectrum, with applications in NDT for aeronautic and space industry and optical metrology for the measurement of deformation of space reflectors in thermal vacuum conditions.

Aïcha Medjahed obtained her engineering degree in technical optics from the Institut d'Optique et Mécanique de Précision, University Ferhat Abbas, Sétif1, Algeria. She received her doctoral degree in physical optics and photonics in 1990 from the University of Louis Pasteur (Strasbourg) France. She is professor of physical optics at the University of Ferhat Abbas Sétif at the Institut d'Optique et Mécanique de Précision since 1991. Her current areas of interest are speckle metrology and biotechnology.

Ivan de Oliveira graduated in physics from the São Paulo State University—UNESP and received his PhD in 2005 from the University of Campinas (UNICAMP) of Brazil. Since 2011, he has been responsible for the Laboratório de Óptica of the School of Technology (UNICAMP). His present areas of interest are photorefractive materials, photosensitive materials, and holographic interferometry.

Marc P. Georges received his licence in physics at Université catholique de Louvain in 1989. He joined the CSL in 1990 and received his PhD in 1998. Since 2006 he has been responsible for the CSL Laser and NDT laboratory. He leads research and development in optical metrology by analog and digital holography and NDT of composites with thermography and laser ultrasonics. He is a member of SPIE, OSA, and SFO.